We are IntechOpen, the world's leading publisher of Open Access books Built by scientists, for scientists

6,900
Open access books available

185,000
International authors and editors

200M
Downloads

Our authors are among the

154
Countries delivered to

TOP 1%
most cited scientists

12.2%
Contributors from top 500 universities

WEB OF SCIENCE™

Selection of our books indexed in the Book Citation Index in Web of Science™ Core Collection (BKCI)

Interested in publishing with us?
Contact book.department@intechopen.com

Numbers displayed above are based on latest data collected.
For more information visit www.intechopen.com

Chapter 1

Optical Signal Processing for High-Order Quadrature-Amplitude Modulation Formats

Guo-Wei Lu

Additional information is available at the end of the chapter

http://dx.doi.org/10.5772/61681

Abstract

In this book chapter, optical signal processing technology, including optical wavelength conversion, wavelength exchange and wavelength multicasting, for phase-noise-sensitive high-order quadrature-amplitude modulation (QAM) signals will be discussed. Due to the susceptibility of high-order QAM signals against phase noise, it is imperative to avoid the phase noise in the optical signal processing subsystems. To design high-performance optical signal processing subsystems, both linear and nonlinear phase noise and distortions are the main concerns in the system design. We will first investigate the effective monitoring approach to optimize the performance of wavelength conversion for avoiding undesired nonlinear phase noise and distortions, and then propose coherent pumping scheme to eliminate the linear phase noise from local pumps in order to realize pump-phase-noise-free wavelength conversion, wavelength exchange and multicasting for high-order QAM signals. All of the discussions are based on experimental investigation.

Keywords: Optical Signal Processing, Nonlinear Optics, Advanced Optical Modulation Formats, Quadrature Amplitude Modulation

1. Introduction

Recently, digital signal processing (DSP) is playing an increasingly important role in coherent detection for reconstructing the complex field of signal and compensating for the transmission impairments. It dramatically simplifies the reception of multi-level and multi-dimensional modulation formats such as high-order quadrature amplitude modulation (QAM), thus making high-order QAM become a promising and practical approach for achieving higher bit rate and higher spectral efficiency. However, optical signal processing is still highly desirable

INTECH
open science | open minds

© 2015 The Author(s). Licensee InTech. This chapter is distributed under the terms of the Creative Commons Attribution License (http://creativecommons.org/licenses/by/3.0), which permits unrestricted use, distribution, and reproduction in any medium, provided the original work is properly cited.

and appreciable in order to overcome the electronics bottlenecks, support the transparency and ultra-fast processing in future optical networks. As basic optical network functionalities, all-optical wavelength conversion, wavelength data exchange, and wavelength multicasting play important roles in the all-optical networks to enhance the re-configurability and non-blocking capacity, and facilitate the wavelength management in future transparent optical networks.

On the other hand, recently, lots of advanced modulation formats like single-carrier high-order QAM like 64QAM [1–5] or multi-carrier optical orthogonal frequency-division multiplexing (OFDM) have been introduced and realized in optical communications for enabling spectrally-efficient and ultra-fast optical transmissions. It is desirable to exploit optical signal processing schemes suitable for these advanced optical modulation formats. However, for these high-order QAM signals, the increasing number of states in the constellation makes the signal more sensitive to the intensity and phase noise. It is imperative to suppress phase noise in optical signal processing subsystems to allow compatibility phase-noise sensitive high-order QAM formats.

As one of the basic optical signal processing techniques, several all-optical wavelength conversion (AOWC) schemes have been demonstrated to realize AOWC functions of OFDM, 8ary phase-shift keying (8PSK), 16QAM, and 64QAM by using the second-order nonlinear effect in periodically-poled Lithium Niobate (PPLN) waveguide [6, 7], four-wave mixing (FWM) in highly-nonlinear fibers (HNLF) [8, 9], semiconductor optical amplifier (SOA) [10–12], or silicon waveguide. However, the implementation penalty of such subsystems varies from 2dB to 4dB at bit-error rate of 10^{-3} [9, 12], which is non-negligible for optical networks, especially when multiple wavelength conversion nodes are included in the networks. The distortions introduced in the AOWC mainly originate from: i) the phase noise from the pumps due to the finite laser linewidth, referred to as linear phase noise; and ii) other undesired nonlinear distortions or crosstalk co-existed in the nonlinear process, called as nonlinear phase noise or distortion. To suppress the linear phase noise from pumps, the straightforward way is to use narrow-linewidth lasers, such as external-cavity laser (ECL) or fiber laser (FL), as pump sources. However, it increases the implementation cost. On the other hand, since the nonlinear media in the sub-system is operated in the nonlinear operation region, expect the dominant nonlinear effect utilized for implementing optical signal processing functionalities, it is highly possible that other undesired nonlinear effects co-occur in this process, thus deteriorating the quality of the converted signal. For example, for the wavelength conversion based on the FWM in SOA, additional distortion from cross-gain modulation, cross-phase modulation (XPM), and self-phase modulation (SPM) may deteriorate the converted signal, while in the wavelength conversion based on FWM in HNLF, additional undesirable distortions are mainly from stimulated Brillouin scattering (SBS), SPM or XPM. High-order QAMs, especially going up to 32QAM, 64QAM or beyond, exhibit more sensitive to nonlinear phase noise like SPM or XPM [13]. Therefore, in order to realize a high-quality all-optical wavelength conversion (AOWC) sub-system for high-order QAMs, it is essential to optimize the system performance of AOWC through effective monitoring approach to suppress the distortion introduced by extra undesired nonlinear distortions. In this chapter, it is categorized into two

http://dx.doi.org/10.5772/61681

parts. In the first part, the effective monitoring approach is discussed to avoid the undesired nonlinear phase noise and distortions in the optical signal processing subsystem to enable superior performance [14]. Then, a coherent pumping scheme is proposed and discussed in the second part to implement the pump-phase-noise-free wavelength conversion, wavelength exchange, and wavelength multicasting for high-order QAM signals. Figure 1 summarizes the main topics which will be discussed in this book chapter.

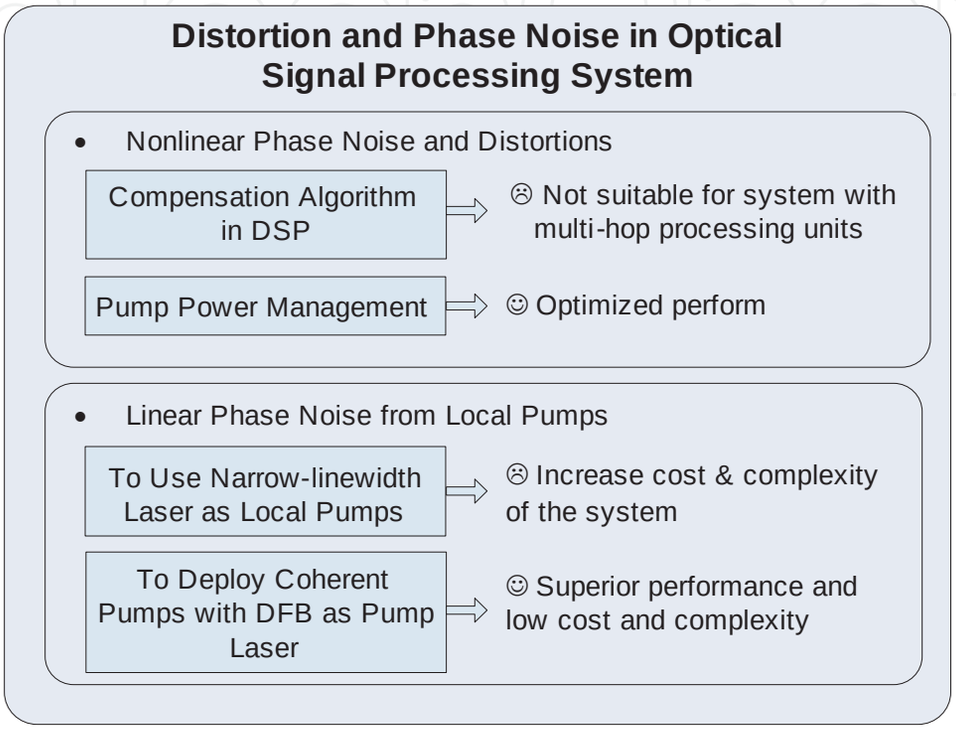

Figure 1. Topics to be discussed in this book chapter.

2. Performance optimization of wavelength conversion of high-order QAM signals

It is well-known that for high-order QAM signals, the increasing number of states in the constellation makes them more sensitive to the intensity and phase noise. Previously, power penalties of around 4 dB at 5Gbaud [12], and 2 dB at 21Gbaud [9] were experimentally demonstrated for the converted 64QAM at bit-error rate (BER) of 10^{-3}. As shown in Fig. 3, to implement the AOWC for high-order QAMs, a simple degenerate FWM in HNLF is deployed. Input QAM signal serves as probe, while a CW pump works as pump in AOWC. The phase of the converted signal follows the phase relationship: $\theta_{idler}=2\theta_{pump}-\theta_{probe}$, where θ_{idler}, $\theta_{pump,}$ and θ_{probe} are the phase of the idler, pump and probe, respectively. In order to implement an AOWC for QAM signals with minimal power penalty, the phase and intensity noise from both pump and probe should be suppressed. Since high-order QAM signals are sensitive to the

phase noise in the system, to avoid the introduced linear phase noise from pump, it is preferred to deploy narrow linewidth light sources for the pump source. In the following experimental demonstration, a tunable external cavity laser (ECL) with the linewidth of around 100 kHz is employed as the light source of the input QAM signal (probe). On the other hand, two fiber lasers (FLs) with a linewidth of around 10 kHz are used as light sources for pump and local oscillator (LO) at the coherent receiver. Since a narrow-linewidth FL was deployed as pump source, the linear phase noise from pump was negligible.

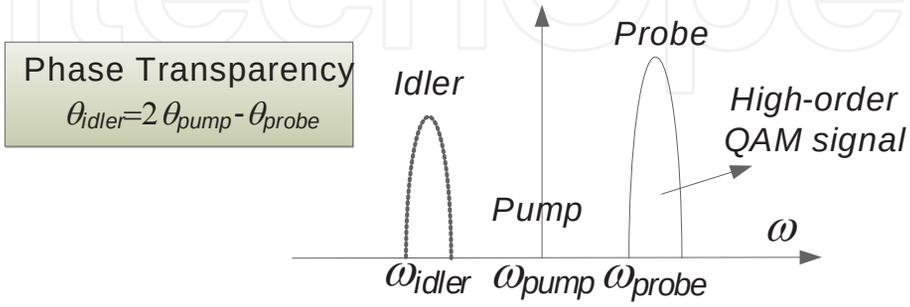

Figure 2. Operation principle of wavelength conversion using FWM in HNLF.

In the AOWC subsystem based on FWM in HNLF for high-order QAM signals, the main nonlinear distortions in the converted signal are mainly from the following sources:

1. SPM from the probe signal: Since the input QAM signal, i.e. the probe, exhibits multilevel in amplitude, in the nonlinear operation condition, the probe may experience SPM. The nonlinear phase noise will then be transferred to the converted signal through FWM and finally deteriorate the converted signal. Therefore, it is critical to manage the launched power of probe to avoid the degradation in the converted QAM signal caused by the probe-introduced SPM. However, it will sacrifice the conversion efficiency. There is a tradeoff between conversion efficiency and the quality of the converted signal in the performance optimization.

2. XPM from the pump signal: As discussed in [15,16], with limited optical signal-to-noise ratio (OSNR) in pump, the amplitude noise in pump may distort the converted signal by introducing nonlinear phase noise through XPM effect. In our experiment, a FL is used as the pump source. Thanks to the low relative intensity noise (RIN) of the FL, the OSNR of pump source is measured as around 57 dB, which avoids the pump-induced nonlinear phase noise.

3. SBS from the pump signal: In AOWC subsystems based on FWM in HNLF, SBS limits the conversion efficiency unless the pumps' linewidth is broadened to increase the SBS threshold. In an AOWC based on degenerate single-pump FWM, if intentionally applying phase dithering on the pump, it will deteriorate the converted QAM signals. Although it has been shown that the phase dithering could be compensated for at the coherent digital receiver by DSP [17], the applied phase dithering will be accumulated in the converted signal as distortions and be further transferred to the next node,

which is not suitable for multi-hop optical networks. In our experiment, thanks to the short length (150 m) and high nonlinearity (nonlinear coefficient: 18/W/km) of the deployed HNLF, the measured SBS threshold is around 24 dBm, which allows a high launching power even without applying additional phase dithering. However, the optimization of the pump power is required in order to avoid the SBS distortion in the pump.

As discussed above, the main undesired nonlinear components in the AOWC based on degenerate FWM in HNLF are from SPM of the input QAM (probe) and SBS of the CW pump. In order to eliminate these deleterious components in the converted signal, the launched pump and probe power should be well managed.

2.1. Experimental investigation

Figure 3 depicts the experimental setup used to achieve the AOWC of 36QAM and 64QAM through FWM in HNLF. Since high-order QAM signals are sensitive to the phase noise in the system, it is preferred to employ narrow-linewidth light sources in the experiment, especially for the pump source. Owing to the lack of instruments in the lab, in the experiment, a tunable ECL with a linewidth of around 100 kHz was deployed as a light source of the input QAM signal in the experiment, whereas two FLs with a linewidth of around 10 kHz worked as light sources for the pump and LO at the coherent receiver. To synthesize optical QAM signals, the light from the ECL, operating at 1551.38 nm, was modulated by a single in-phase/quadrature (IQ) modulator, which had a 3 dB bandwidth of around 25 GHz, and a 3.5 V half-wave voltage. Two de-correlated 6- or 8-level driving signals originating from pseudorandom binary sequence (PRBS) streams with a length of 2^{15}–1 from an arbitrary waveform generator (AWG) were used to drive the IQ modulator for generating optical 36QAM or 64QAM, respectively. After power amplification, the QAM signal was combined with amplified CW light at 1551.95 nm, and was then fed into a 150 m length of HNLF having an attenuation coefficient of 0.9 dB/km, a nonlinear coefficient of 18/W/km, a zero-dispersion wavelength of 1548 nm, and a dispersion slope of around 0.02 ps/nm^2/km. Note that, due to the inability to tune the wavelength of the FLs used in the experiment, wavelengths of the probe signal and pump could not be set for the optimum FWM efficiency. Nevertheless, owing to the high nonlinear effects and flat-dispersion-profile of the employed HNLF, the experimental results showed high conversion efficiency, which can ensure the superior performance of the converted signal. The produced idle signal at the wavelength of 1552.52 nm was filtered out and then led to the phase-diversity intradyne coherent receiver for the coherent detection and for BER measurement. The coherent receiver included an LO, a 90 degree optical hybrid device, and two balanced photo-detectors (PDs). After detection by the balanced PDs, the data was digitized at 50GSamples/s by employing a digital storage oscilloscope (Tektronix DP071254) which has the analog bandwidth of 12.5 GHz. The captured data was processed offline through the DSP that included compensation of skew, IQ imbalance, power, data resampling, linear equalization using the finite impulse response (FIR) filtering, carrier phase recovery, and the final hard-decision circuits. 89,285 symbols were used for the BER measurement.

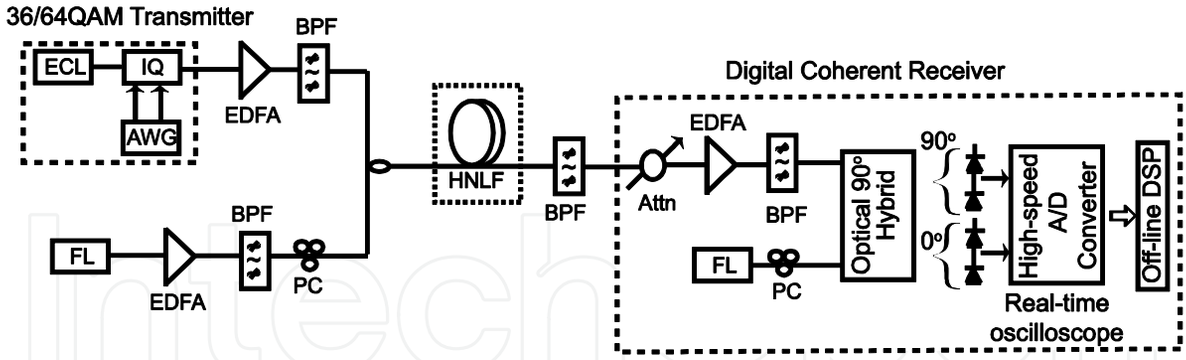

Figure 3. Experimental setup of the wavelength conversion of 36QAM and 64QAM signals.

2.1.1. AWOC of 36QAM

In order to eliminate possible deleterious components in the converted signal, the launched pump and probe power should be well managed. Figure 4(a) shows the measured EVMs and BERs at the received OSNR of around 25 dB when the probe power was tuned from 7 to 15 dBm and the pump power was fixed at around 20dBm. An improvement in both the EVMs and BERs of the converted 36QAM was observed with an increase in the probe power up to around 11 dBm. After the inflection point (around 11 dBm), both EVMs and BERs increased with the increase of the probe power, which was attributed to the SPM of probe in the nonlinear process. Therefore, we considered setting the probe power to around 11 dBm to avoid the SPM introduced in the probe. As previously mentioned, another main source of distortion is the SBS of the pump in AOWC. To optimize the pump power, we also measured the corresponding EVMs and BERs when the probe power was fixed at 11 dBm and the pump power was tuned from 15 dBm to 23 dBm (Fig. 4(b)). As the launched pump power increased, EVMs and BERs showed similar behavior. We found that it was better to operate the pump power in the range of 17.5–22 dBm. At the pump power of 15.4 dBm, the constellations were relatively noisy due to the low conversion efficiency. However, once the pump power was increased to 22.9 dBm, distortion from SBS started to appear in the measured constellation, acting mainly as intensity noise. To obtain the optimal performance, we set the pump power at 20 dBm in the AOWC of 36QAM. While monitoring the converted 36QAM, EVMs and BERs showed consistent behavior when tuning the probe and pump powers.

As we discussed previously, the optimal pump and probe power were 20 dBm and 11 dBm for the AOWC of 36QAM. The corresponding optical spectrum under the optimal condition is shown in Fig. 5(i), where a conversion efficiency of about −15 dB was obtained compared with the input probe power. Under the optimal operating condition, the BER performance was measured as the function of OSNR at 0.1 nm for both input and converted signals, and shown in Fig. 5(ii). For the input QAM signals, the power penalty of around 2 dB was obtained compared with theoretical BER measurement at the BER of 10^{-3}, which is better than the previously-reported QAM transmitters [2]. The power penalty is mainly owing to the imperfectness of the transmitter. With respect to the input QAM, a negligible power penalty (<0.3

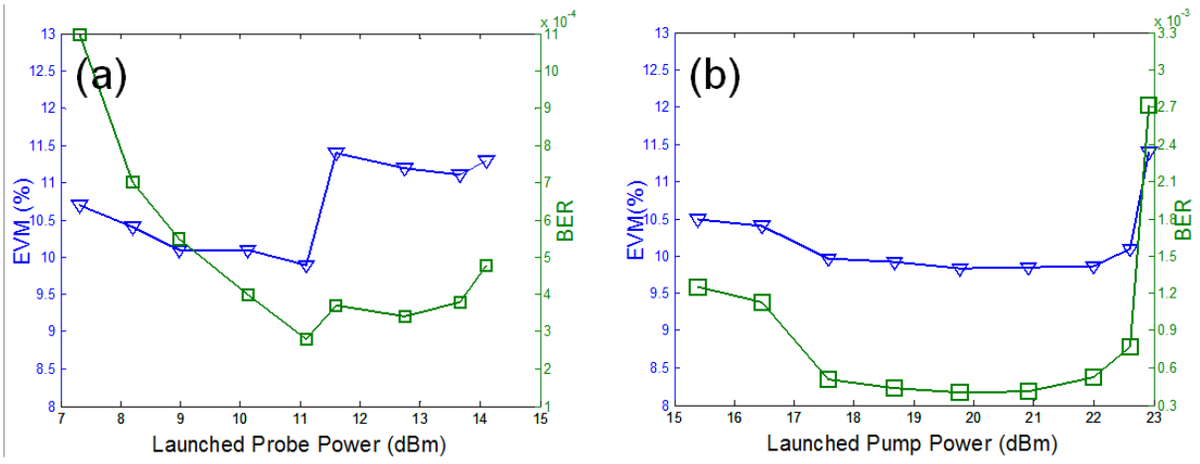

Figure 4. Measured EVM (triangles) and BER (squares) results of the converted 36QAM signals (**a**) when tuning probe power from 7 to 15 dBm, (**b**) when tuning pump power from 14 to 23 dBm.

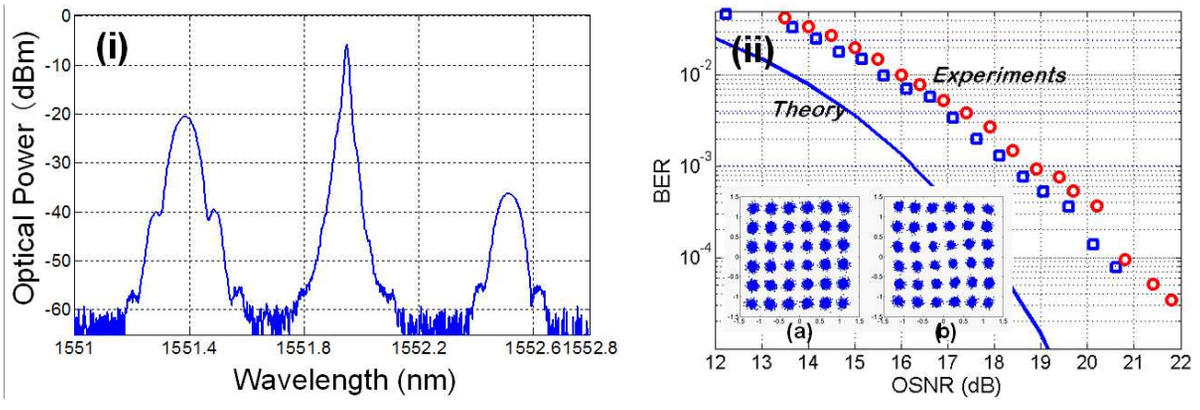

Figure 5. (**i**) Measured optical spectrum in the optimal condition, (**ii**) measured BER as function of the received OSNR (0.1 nm). Insets: (**a**) input and (**b**) converted 36QAM signals.

dB) was observed at a BER of 10^{-3}. The measured constellations of the input and converted 36QAM are shown in the insets of Fig. 5(ii), where the received OSNR was around 35 dB.

2.1.2. AWOC of 64QAM

To optimize the performance of AOWC for 64QAM, measurements similar to those described above were performed. Figure 6 (a) depicts the measured EVMs and BERs at the received 25 dB OSNR when the probe power was tuned from 7 to 15 dBm and the pump power was fixed at around 20 dBm. The increase in the launched probe power decreased the BER of the converted signal to around 12.2 dBm owing to the improved OSNR of the converted signals. When the probe power was increased further, the BER started to increase, attributed to the introduced SPM in the probe signal. The BER results with different probe powers suggested to operate the probe power in the range of 9 to 14 dBm. Furthermore, the measured constellations offered a more perceptive and precise approach for optimizing the performance. The EVMs with the various probe powers were calculated and are plotted in Fig. 6(a). With the

increase of the probe power, both BER and EVM results show similar trends. However, according to the EVM and BER results, different optimum probe powers of around 9.2 dBm and 12.4 dBm were obtained, respectively. When the launched probe power was increased to around 12.4 dBm, SPM-induced distortion became visible in the constellation, causing the increase of EVM. However, the SPM-induced spiral rotation in the constellation happens to enlarge the symbol distance between symbols, thus decreasing the BER. Therefore, these results suggested that, to optimize the performance of AOWC, it would be effective to monitor the constellation or EVM, which gives a more intuitive and proper means to optimize the AOWC performance, in order to eliminate the extra undesired nonlinear phase noise introduced in the process.

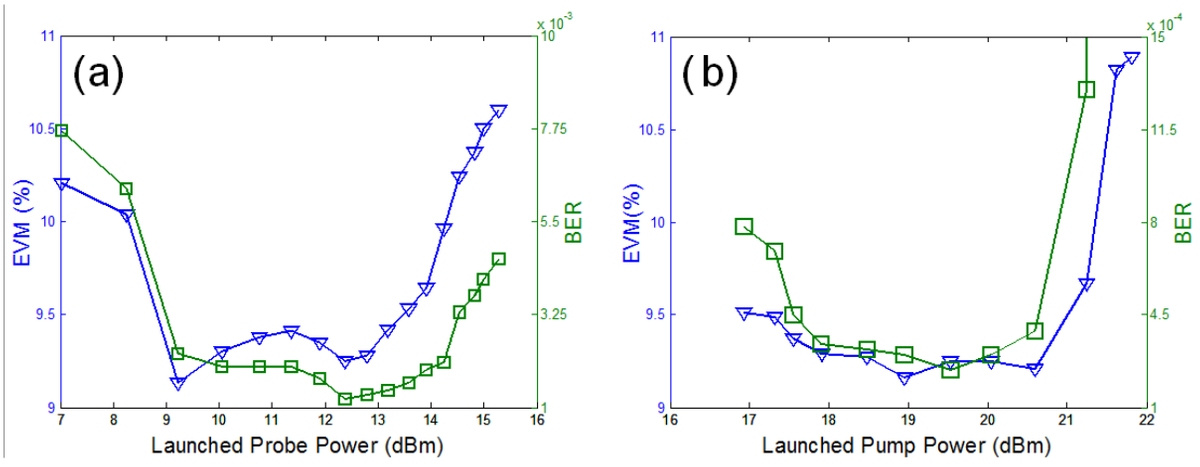

Figure 6. Measured EVM (triangles) and BER (squares) results of the converted 64QAM signals (**a**) when tuning probe power from 7 to 15 dBm, (**b**) when tuning pump power from 17 to 21 dBm.

For pump power optimization, the EVM and BER results were measured when the launched pump power was increased from 17 to 22 dBm, whereas the pump power was set at around 9 dBm. The measurement was done for optimizing the pump power and is shown in Fig. 6(b). Similar behavior was obtained for the measured EVM and BER values when the pump power was increased. In order to avoid the distortion owing to the SBS, we considered to set the pump power in the range of 17.5–20.5 dBm. It is clear that a high pump power was helpful for obtaining high conversion efficiency, therefore, resulted in a sufficient OSNR for the converted signal. Thus, in this experiment, the pump power was optimized to 20 dBm, which resulted in a conversion efficiency of about -15 dB and also ensured that there was no SBS distortion introduced for the converted signal. The distortion from SBS acted mainly as amplitude noise in the constellations, and became severe once the pump power was increased to more than 20.5 dBm.

To achieve the optimal performance of AOWC for 64QAM signal, the pump and probe power were set at 20 dBm and 9 dBm, respectively. A conversion efficiency of around −15 dB is obtained, as shown in Fig. 7(i). Under the optimized conditions, the BER performance as a function of OSNR was shown in Fig. 7(ii). The implementation penalty compared with the theoretical BER curve was around 2.8 dB for 64QAM, at a BER of 10^{-3}, which is much better

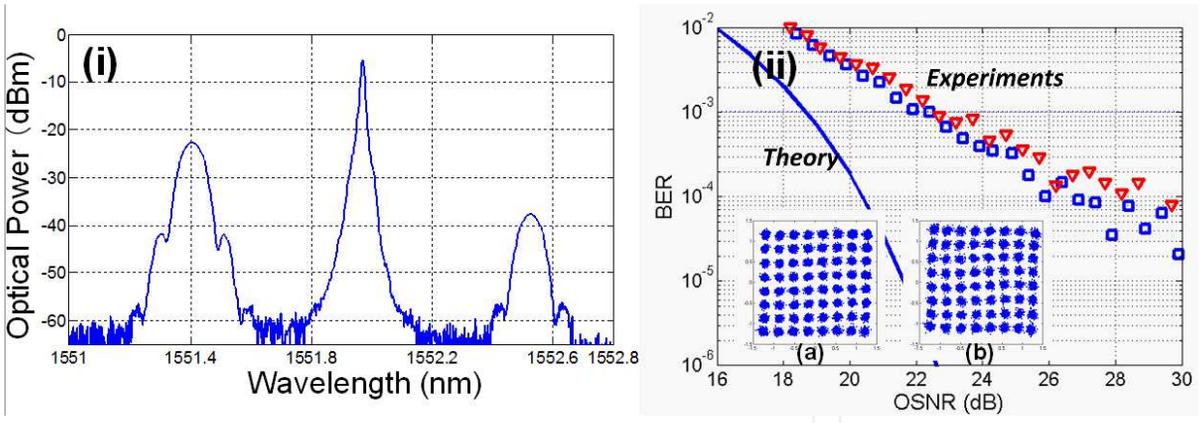

Figure 7. (**i**) Measured optical spectrum in the optimal condition, (**ii**) measured BER as function of the received OSNR (0.1 nm). Insets: (**a**) input and (**b**) converted 64QAM signals.

than those of the previously-reported 64QAM transmitters in [3–4]. Similar to that performance of 36QAM AOWC, a negligible power penalty of <0.3 dB was observed with the respect to the input signal at a BER of 10^{-3} after the conversion. The obtained constellations of the input and converted high-order QAMs at around 35 dB received OSNR and are shown in the insets of Fig. 7(ii).

2.2. Summary

We have experimentally demonstrated the AOWC of optical 10-Gbaud (50 Gbps) 36QAM and (60 Gbps) 64QAM through a degenerate FWM effect in HNLF with a power penalty of less than 0.3 dB at a BER of 10^{-3}. In order to optimize the AOWC performance, the converted high-order QAM signals were evaluated by measuring the BER and constellations, i.e., EVM. Since EVM showed higher sensitivity in the presence of nonlinear phase noise, the results suggested the effectiveness of optimizing the AOWC performance by monitoring EVM, rather than BER, especially for high-order QAM signals.

3. Pump-phase-noise-free optical signal processing

The previous session mainly focuses on how to avoid or suppress the nonlinear noise or distortion in optical signal processing. In this session, the focus is to exploit the approach to eliminate the linear phase noise from the local pumps deployed in optical signal processing subsystems. In optical signal processing subsystems, such as wavelength conversion, wavelength exchange or wavelength multicasting, it is inevitable to deploy local pump sources to realize the optical signal processing functionalities. As we discuss before, the linear phase noise from local pumps may introduce phase noise or distortion to the converted signal in optical signal processing subsystem. The most straightforward way is to deploy narrow-linewidth lasers as pump sources. However, it increases the implementation cost of the systems. We will present our proposed coherent pumping scheme. Thanks to the phase noise cancelling effect using this coherent pumping, it allows the use of low-cost distributed feedback (DFB) lasers

as pump sources, and at the same time, ensures the superior performance since it is free of the phase noise from pumps. Here we will demonstrate several pump-phase-noise-free optical signal processing subsystems for high-order QAM signals, including: (a) pump-phase-noise-free wavelength conversion and wavelength exchange for high-order QAMs signals using cascaded second-order nonlinearities in PPLN [18, 19]; and (b) pump-phase-noise-free wavelength multicasting of QAM signals using FWM in HNLF [20].

3.1. Pump-phase-noise-free wavelength conversion and wavelength exchange in PPLN

Figure 8 depicts the operation principle of the pump-linewidth-free AOWC. It is based on cascaded second-order nonlinearity in PPLN. Two pumps at ω_{p1} and ω_{p2} are allocated at one side of quasi-phase-matching (QPM) wavelength of PPLN, whereas input signal at ω_1 is placed symmetrically with pump at ω_{p1} with respect to QPM wavelength. After AOWC, the input signal at ω_1 is shifted to the frequency ω_2, with $\omega_2=\omega_{p1}-\omega_{p2}+\omega_1$, where ω_{p1}, ω_{p2} and ω_1 are the frequencies of pump1, pump2, and the input signal, respectively. It is typically employed for performing the data exchange between the two input wavelengths [13], i.e. wavelength exchange. The frequencies ω_{p1} and ω_1 have to be arranged symmetrically with the respect to the PPLN's quasi-phase-matching (QPM) wavelength in order to satisfy the phase matching condition and for increasing the conversion efficiency. With the non-depletion assumption, linear mapping between the input and output relationship in complex amplitudes and phase are given by equations (1) and (2), respectively.

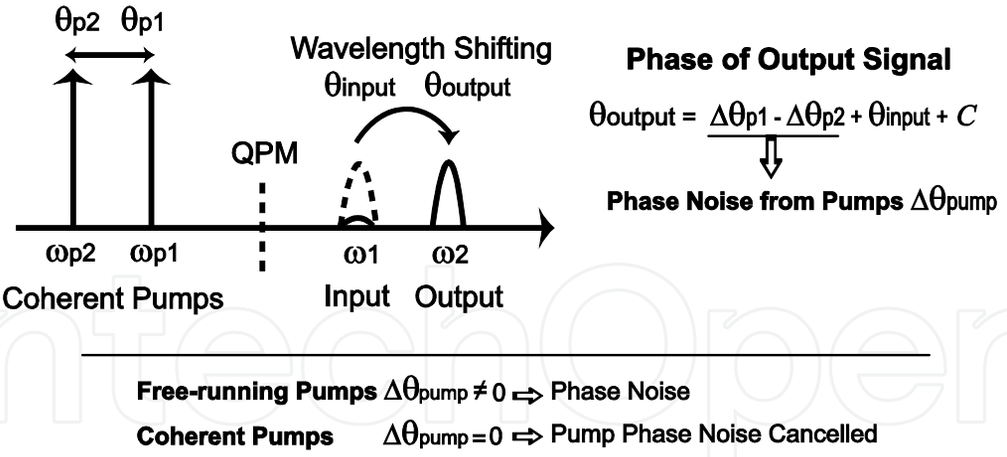

Figure 8. Operation principle of the pump phase-noise cancellation using coherent pumping.

$$A_{\omega_2} \propto A_{\omega_1} \cdot A^{*}_{\omega_{p2}} \cdot A_{\omega_{p1}} \tag{1}$$

$$\theta_{output} = \theta_{input} + \Delta\theta_{p1} - \Delta\theta_{p2} + C = \theta_{input} + \Delta\theta_{pump} + C \tag{2}$$

where θ_{output}, θ_{input}, $\Delta\theta_{p1}$, $\Delta\theta_{p2}$, and *C* are the phase of the converted and input signals, the phase noise from pump1 and pump2, and a constant term, respectively, and $\Delta\theta_{pump} = \Delta\theta_{p1} - \Delta\theta_{p2}$. Note that the phase information in each pump is transparently transferred to the converted signal as a subtraction term between them. In order to avoid additional phase noise introduced in the process, the phase noise term from pumps, $\Delta\theta_{pump}$, should be minimized. If the pumps are synthesized by a two-tone generator (TTG) from a single laser source, the phase noise from pumps is eliminated in the converted signal, i.e. $\Delta\theta_{pump}=0$. Hence, the wavelength conversion becomes free of the phase noise from pumps, allowing the use of lower cost lasers and at the same time ensuring a superior performance in terms of noise performance. The TTG may be constructed using either Mach-Zehnder modulators driven by a RF clock, or an optical frequency comb followed by an optical spectrum shaper. The two-tone spacing could vary from a fraction of nanometer to several nanometers, making it possible to cover a relative wide conversion range in the OWC. The TTG generated from a filtered optical frequency comb is more suitable and practical for the OWC based on HNLF.

3.1.1. Pump-phase-noise-free AOWC in PPLN

The experimental set-up is depicted in Fig. 6, showing OWC scheme of 16 and 64 QAM signals. A 5kHz linewidth FL at the wavelength of 1552.52 nm was deployed as the light source to minimize the phase noise from the input signal. And then the light was modulated by an in-phase/quadrature (IQ) modulator for generating QAM signals. The two de-correlated 4- or 8-level driving electronics derived from 10-Gbaud PRBS streams with the length of 2^{15}–1 were generated from an arbitrary waveform generator (AWG) to drive the IQ modulator, which has a $V\pi$ of 3.5 V and an optical bandwidth of around 25 GHz. Two different pump configurations were adopted for comparison. The two pumps were generated from a single laser source at the wavelength of 1548.08 nm using a TTG in the coherent pump configuration, which consisted of a high extinction-ratio (ER) optical modulator driven by a 25-GHz RF clock. The high-ER modulator was made up on the x-cut $LiNbO_3$ substrate with two embedded active trimmers in each arm and it has the extinction ratio of up to 60 dB. The two phase-correlated coherent pumps were obtained with the 50-GHz frequency separation with a >40-dB spurious suppression ratio. For the case of free-running pumping, two independent free-running lasers at the wavelengths of 1547.88 and 1548.28 nms were used as pumps with 50-GHz spacing. For each of the configurations, we tried either the 500-kHz linewidth ECLs or the 3.5-MHz linewidth DFBs as the laser sources for the pumps.

The optical spectra with and without pumps for wavelength conversion of 64QAM signals after the PPLN are shown in Fig. 10. Similar conversion efficiency (CE) and signal depletion (SD) were obtained for the both free-running pumps (ECL/DFB) and coherent two-tone pumps (ECL/DFB). Here, the CE is defined as the power ratio between the converted signal to the input signal after the PPLN. On the other hand, the SD is the power ratio of the input signal after the PPLN when the both pumps were switched OFF and ON, respectively. The total pump power launched into the PPLN was set to the maximum value of about 28.8 dBm (25.8 dBm for each pump) to maximize both CE and SD, where CE of -6.5 dB and SD of 25 dB were obtained with input signal power of 6 dBm.

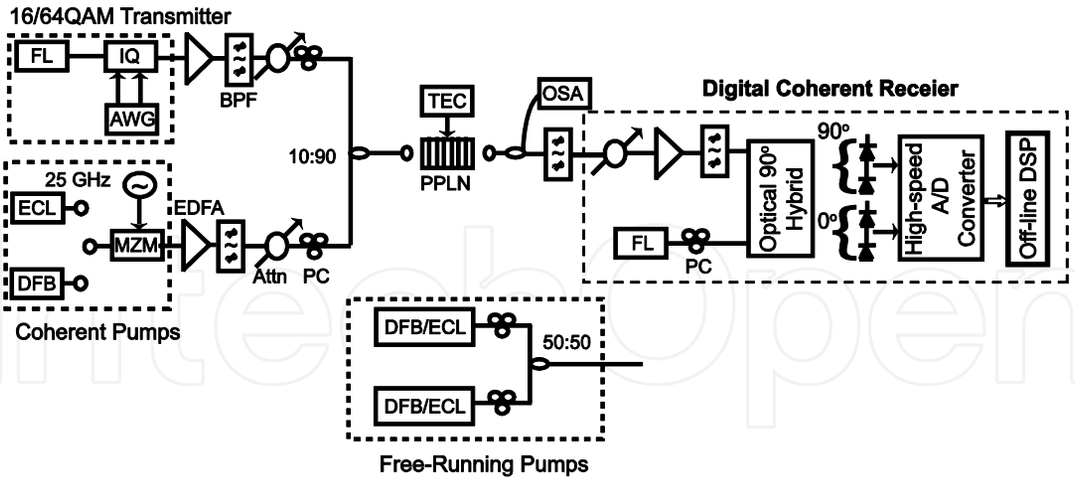

Figure 9. Experimental set-up for AOWC of 16QAM and 64QAM signals.

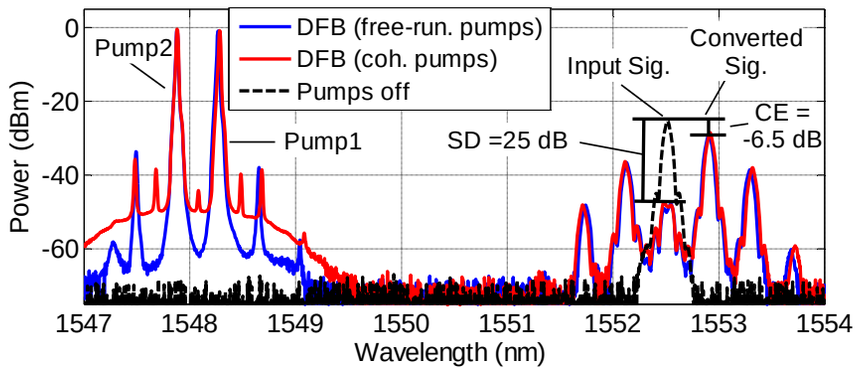

Figure 10. Optical spectra measured after PPLN when performing OWC of 64QAM with DFB pump lasers in both free-running and coherent configurations.

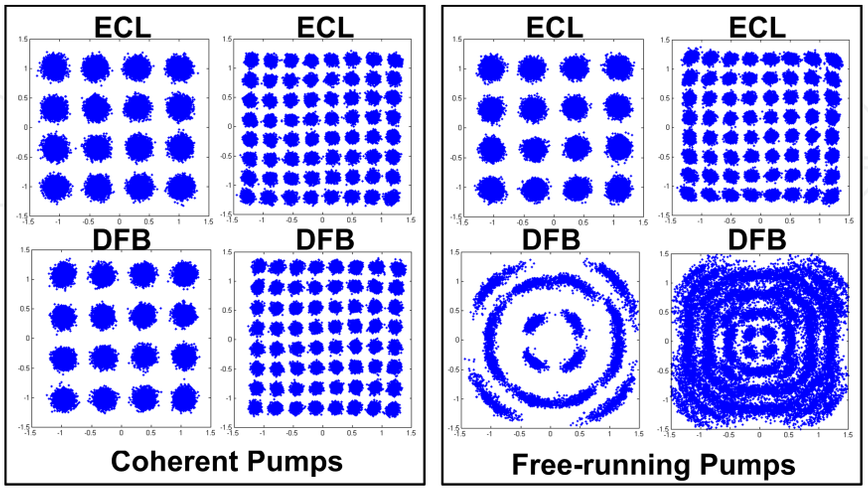

Figure 11. Measured QAM constellations using ECL and DFB pump lasers in coherent two-tone and free-running configurations (16QAM: OSNR=18 dB, 64QAM: OSNR =34 dB).

The constellations of the converted 16/64QAMs signals were re-constructed and observed with different pump lasers and pump configurations. As shown in Fig. 11, for either ECL or DFB pump laser, clear constellations are observed with coherent two-tone pumps. On the other ways, with the ECL pump lasers in free-running configuration, symbol rotation in phase starts to turn into obvious in the 64QAM constellation owing to the additional phase noise from the free-running ECL pumps. Furthermore, the presence of even larger pump phase noise causes clear spreading of the symbols around the unit circle for both formats with DFB free-running pumps, which is more severe for the higher amplitude symbols. From the measured BER curves, the results can also be confirmed as a function of optical signal-to-noise ratio (OSNR) at 0.1 nm for both input and converted 16/64QAM signals, as seen in Fig. 12. For both ECL and DFB pump lasers with coherent pump configuration, negligible power penalties of <0.1 dB for 16QAM and <0.3 dB for 64QAM at BER of 10^{-3} are observed with the respect of the input signal at 10Gbaud. Although we can get insignificant power penalty of <0.3 dB at BER of 10^{-3} for 16QAM with ECL as the pump laser, by increasing the modulation level to 64QAM, a 0.5 dB penalty at BER of 10^{-3} and an error floor at around 3×10^{-5} are observed in the case of free-running pumps. Owing to the strong phase noise with the free-running DFB pumps, even at >30 dB OSNR, a BER of around 10^{-2} is observed for 16QAM. The effectiveness of the pump-phase-noise removal in the OWC for high-order QAM with coherent two-tone pumps is verified by the BER and constellation results.

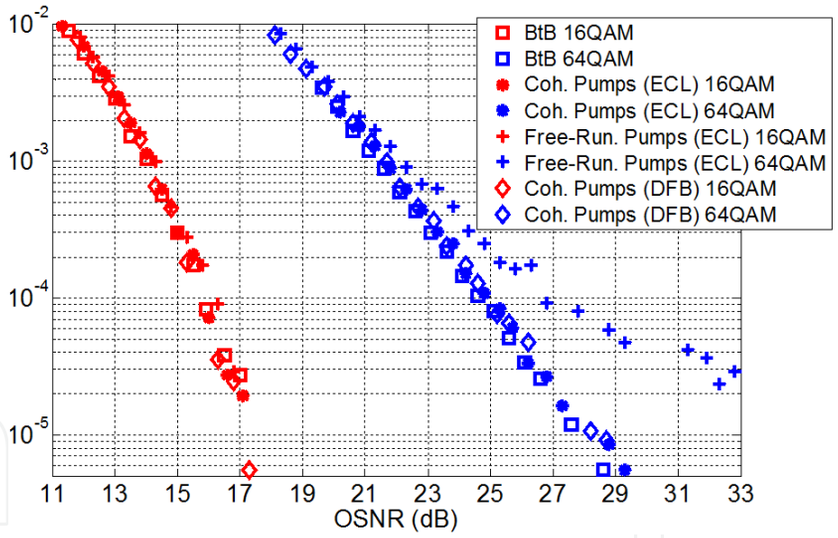

Figure 12. Measured BER vs. OSNR curves for 16/64QAM. Squares: back-to-back (BtB), stars: coherent pumps (ECL), crosses: free-running pumps (ECL), diamonds: coherent pumps (DFB).

3.1.2. Pump-phase-noise-free wavelength exchange in PPLN

Wavelength exchange is a kind of optical signal processing technique to realize bidirectional information swapping between different wavelengths. It consists of simultaneous signal depletion and wavelength conversion processes of two participated channel signals. Each of input signals is power consumed and its corresponding power is shifted to the other wave-

length, finally realizing data exchange between two wavelengths in single device. So far, several works have been demonstrated through non-degenerate FWM in highly-nonlinear fiber [21–24] or cascaded second-order nonlinearities in PPLN waveguide [25–26].

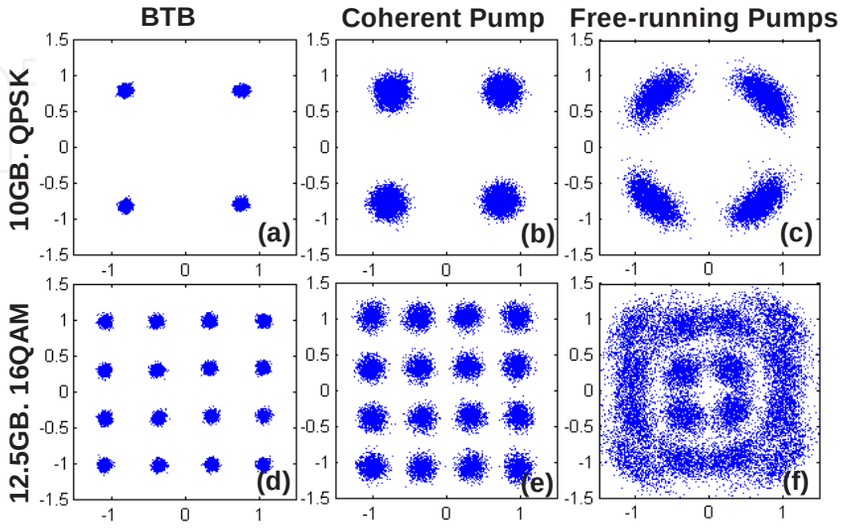

Figure 13. Measured constellations of input and converted signals after wavelength exchange (16QAM and QPSK).

Here, we apply the coherent pumping concept to wavelength exchange to demonstrate pump-phase-noise free wavelength exchange in PPLN. For experimental demonstration, an experimental setup similar to the one shown in Fig. 9 was deployed by adding another input signal. Two input signals modulated in 16QAM and QPSK, respectively were launched to PPLN as input signals for performing wavelength exchange. To evaluate the performance of wavelength exchange, BER and constellations were measured. The constellations of the swapped signals with different pump configurations are depicted in Fig. 13. With coherent pumps, clear constellations are observed for both QPSK and 16QAM. However, with DFB free-running pumps, the presence of pump phase noise causes clear spreading of the symbols around the unit circle with which is more severe for the higher amplitude symbols in 16QAM. It implies that with incoherent DFB pumps, the phase noise from pump severely deteriorates the swapped QAM signals. It can also be confirmed from the measured BER curves as a function of OSNR (0.1 nm) for both input and swapped signals. With coherent DFB pump, around 0.6 dB and 3 dB power penalties at BER of 10^{-3} were obtained for QPSK and 16QAM, respectively. As discussed above, this is mainly attributed to the crosstalk introduced by finite ER (20dB). However, in case of free-running pumps, although it was still possible to obtain BER curve for swapped QPSK, ~3.4-dB penalty and visible error-floor at BER of 5×10^{-4} were clearly observed. Due to the susceptibility of 16QAM against phase noise and crosstalk, it becomes impossible to obtain BER plot for the swapped 16QAM. This verifies the effectiveness of the elimination of the pump phase noise in the OWE for high-order QAM with coherent pumps.

http://dx.doi.org/10.5772/61681

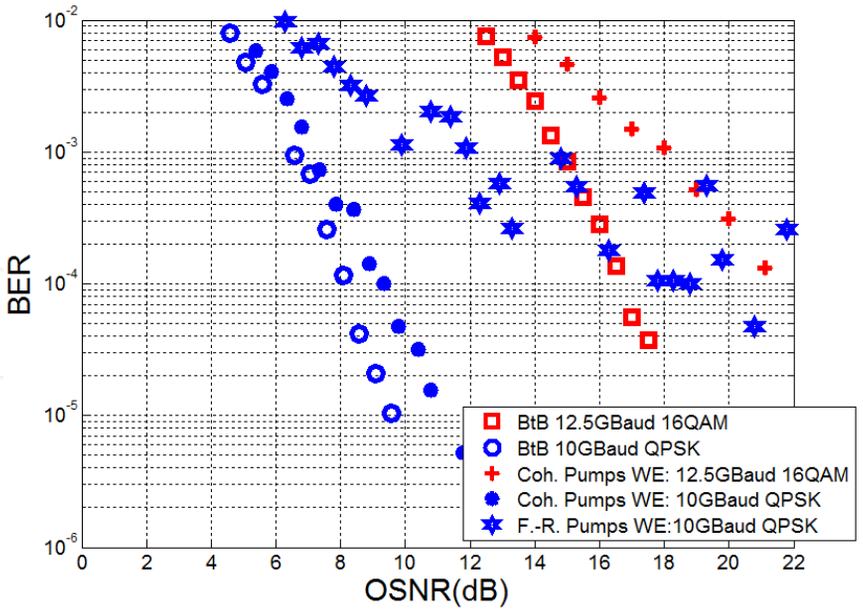

Figure 14. Measured BER vs. OSNR of the input and swapped QAM signals.

3.2. Pump-phase-noise-free wavelength multicasting of high-order QAM by FWM in HNLF

With the emergence of high-bandwidth point-to-multipoint applications such as high-definition Internet TV, big-data sharing, and data center migration, the need for wavelength multicasting has arisen recently to improve the network throughput and decrease the blocking probability in optical networks. Through multicasting, the network wavelength resources could be efficiently and flexibly managed in wavelength division multiplexing networks. Recently, it has also shown the application of wavelength multicasting in the all-optical spectrum defragmentation in elastic optical networks (EON) [27]. All-optical multicast through the nonlinearities in HNLF [28–30], SOA [31] and silicon nanowire waveguide [32] has been reported.

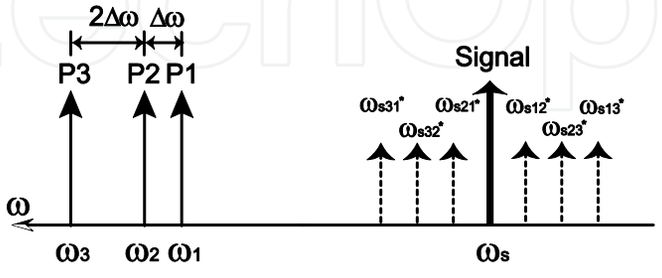

Figure 15. Operation principle of wavelength multicasting based on FWM in HNLF.

With the proposed coherent pumping, it is possible to achieve pump-phase-noise-free wavelength multicasting as well. Figure 15 illustrates the operation principle of the proposed

pump-phase-noise-free wavelength multicasting scheme based on FWM with coherent multi-carrier pump. With the input three pumps at ω_1, ω_2, ω_3, and input signal at ω_s, seven multi-casted channels, including the original input signal, are uniformly generated with a spacing of $\Delta\omega$. The frequency spacing settings of $\Delta\omega$ and $2\Delta\omega$ between ω_1 and ω_2, ω_2 and ω_3 could efficiently avoid the overlapping of spectrum among multicasted channels. It finally leads to a uniform frequency allocation of the multicasted signals alongside of the input signal with a spacing of $\Delta\omega$, which is important to realizing all-optical spectrum defragmentation [27]. The generated six components next to input signal are the non-degenerate FWM components with the frequencies of ω_{sij^*}, where i,j $\in$[1, 2, 3], i≠j, and * symbolizes the conjugate operation. The following equation shows the resultant phase in the multicasted signal at ω_{sij^*}:

$$\theta_{\text{output}} = \theta_{\text{input}} \pm \left(\Delta\theta_{\text{pi}} - \Delta\theta_{\text{pj}}\right) + C = \theta_{\text{input}} \pm \Delta\theta_{\text{pump}} + C \tag{3}$$

where $\Delta\theta_{\text{pump}} = \Delta\theta_{\text{pi}} - \Delta\theta_{\text{pj}}$, and θ_{output}, θ_{input}, $\Delta\theta_{\text{pi}}$, $\Delta\theta_{\text{pj}}$, and C are the phase of the output and input signals, the phase noise from pump i, j where i, j$\in$[1, 2, 3], and a constant term, respectively. When the pumps are coherent in phase, it is obvious that the phase noise from pumps are eliminated in the multicasted signals, i.e. $\Delta\theta_{\text{pump}}=0$. Therefore, the wavelength multicasting becomes tolerant against the phase noise from the pumps. Hence, lower-cost DFB lasers can be used as pump source. In practice, an optical comb with a spacing of $\Delta\omega$ could be employed to generate the coherent multi-carrier pump followed by an optical processor. The optical processor could ether be a liquid crystal on silicon (LCoS) device or cascaded band-pass and notch filters to select coherent carriers with desired spacing. The multicasting scale and the channel spacing of multicasted signals could be simply re-configured by programming the optical processor. The coherent pumping concept has been applied to wavelength conversion to remove the phase noise from the local pumps [18]. It is more beneficial and cost-effective when coherent pumping scheme is extended to multicasting with the flexible coherent multi-carrier pumping.

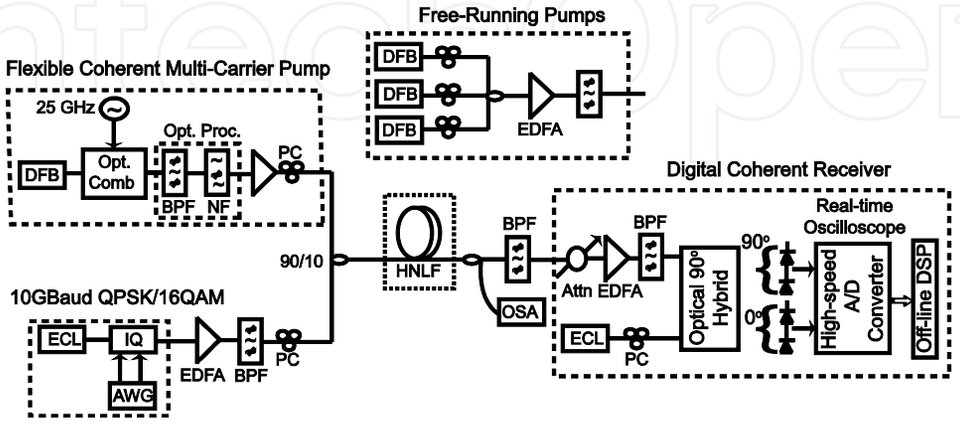

Figure 16. Experimental setup of pump-phase-noise-free 1 to 7 wavelength multicasting based FWM in HNLF.

To verify the proposed pump-phase-noise-free wavelength multicasting, a 1-to-7 multicasting experiment for QPSK and 16QAM signals was conducted with the setup shown in Fig. 16. Different from the setup shown in Fig. 9, a coherent multi-carrier pump is used as pump source, and a piece of highly-nonlinear fiber (HNLF) with length of 150 m is deployed as nonlinear media. The deployed HNLF has an attenuation coefficient of 0.9dB/km, a nonlinear coefficient of 18/W/km, a zero-dispersion wavelength of 1548 nm, a dispersion slope of around 0.02ps/nm^2/km and low β4 (2×10^{-56}s^4/m). Thanks to its high nonlinearity, a short length of HNLF (150 m) is sufficient to achieve the FWM-based wavelength multicasting. To retain the coherence of pumps, the short lengths, low and flat dispersion profile of the deployed HNLF are helpful to maintain the coherence of the pumps when propagating in HNLF. The constellations of the input and multicasted QPSK and16QAM signals with different pumping configurations are shown in Fig. 17. Even using DFB as pump laser, clear constellations are observed with coherent 3-carrier pumping. However, in the case of free-running DFB pumping, for the newly-produced components, clear symbol spreading around the unit circle occurred due to the phase noise from DFB pumps. It happens especially for the outer symbols with higher amplitude in 16QAM. The measured BER curves as function of OSNR (0.1 nm) is depicted in Fig. 18. For both QPSK and 16QAM, less than 0.8 dB power penalty was obtained at BER=10^{-3} for all of the seven multicasted signals with respect to the input signal with coherent pumping. On the other hand, owing to the strong phase noise transferred from the noisy pumps with free-running DFB pumping, error-floor at BER of 1×10^{-3} and 4×10^{-3} was observed for QPSK and 16QAM, respectively. The effectiveness of the elimination of the pump phase noise is verified in the multicasting for QAM signals with coherent multi-carrier pumping.

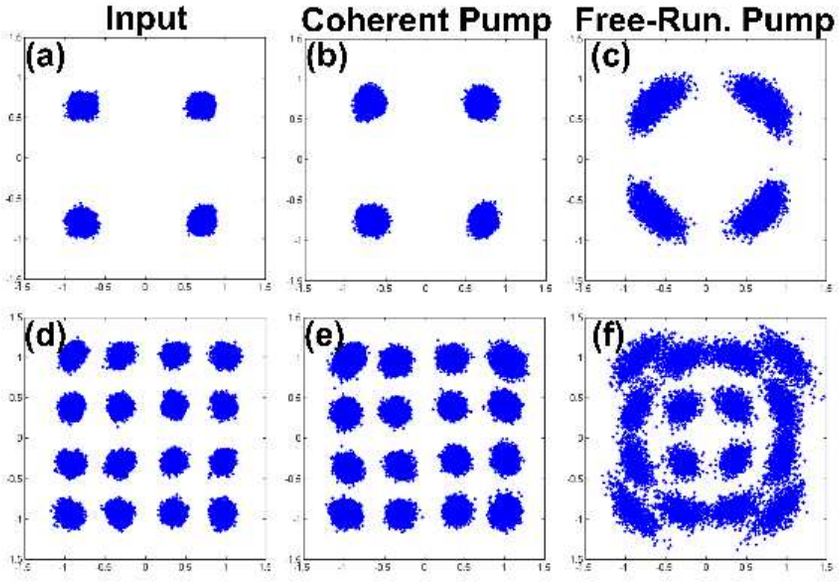

Figure 17. Measured constellations of input and converted signals with coherent pumping and free-running pumping schemes. QPSK: (a)~(c); 16QAM: (d)~(f).

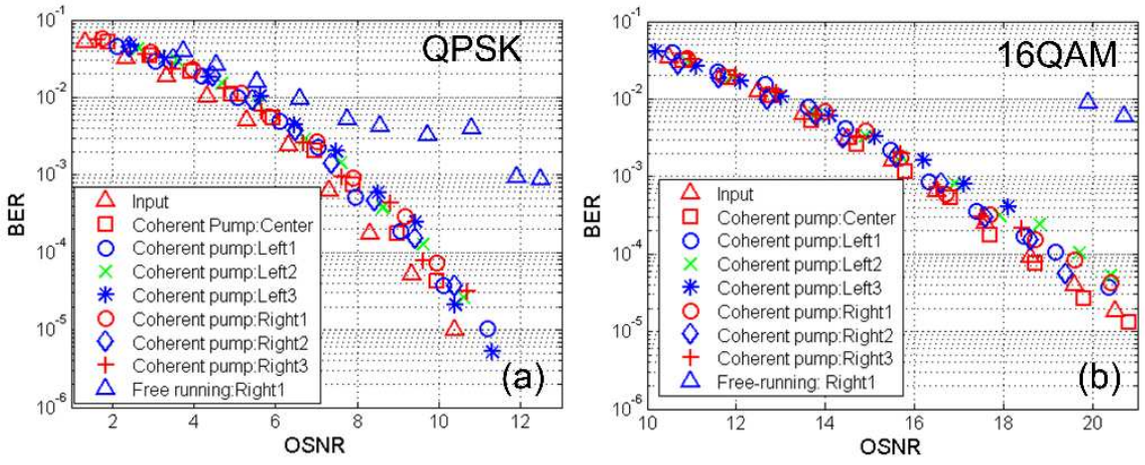

Figure 18. Measured BER vs. OSNR curves for (a) QPSK and (b) 16QAM multicasting systems.

3.3. Summary

In this section, in order to avoid the phase noise introduced from local pumps, coherent pumping concept has been proposed. Through experimental demonstration based on either cascaded second-order nonlinearities in PPLN or third-order nonlinearity in HNLF, we have successfully demonstrated that, even using low-cost noisy DFB lasers as pump source, the phase noise from local pumps could be effectively avoided in optical signal processing for high-order QAM signals, including wavelength conversion, wavelength exchange, and wavelength multicasting. However, in cases of free-running DFB pumps, it is impossible to obtain clear constellations for QAM signals, especially for 16QAM and 64QAM signals, which was significantly deteriorated by the large phase noise from DFB pumps.

4. Future works

To properly conduct optical signal processing for advanced high-order QAM signals, several issues have been addressed in this chapter. We also discussed proposed coherent pumping schemes for realizing the phase-noise-free optical signal processing for high-order QAM signals. For further study and investigation, the following aspects could be considered.

1. Phase-noise-free processing for multi-carrier high-order signals

Here, the study and investigation of phase-noise-free optical signal processing are mainly focusing on the single-carrier high-order modulation formats like high-order QAMs. It is also applicable to the multi-carrier high-order signals, such as coherent optical OFDM (CO-OFDM) with subcarriers modulated in high-order QAMs. Such QAM-CO-OFDM also suffers from the susceptibility against phase noise, especially for CO-OFDM with high-order QAM subcarrier modulations [33]. Therefore, it is highly desirable to further apply the coherent pumping concept to demonstrate the phase-noise-free processing for multi-carrier high-order signals in the near future.

2. Reconfigurable coherent optical multi-carrier

As we point out in the above sections, coherent optical multi-carrier could be produced by an optical comb followed by optical signal processing, which is usually an LCoS-based component. It is cost effective to share multi-carrier for multi-channel signal processing. However, it is still costly to include LCoS-based optical processor in optical signal processing subsystems. Thus, it is interesting to further develop cost-effective coherent multi-carrier with reconfigurable tone number and spacing. It will be one of key components for realizing reconfigurable optical signal processing in the future.

3. Other nonlinear media to realize optical signal processing

The experimental demonstration reported here is mainly focusing on HNLF and PPLN devices. Obviously, it could also be implemented in other nonlinear media like SOA especially quantum-dot SOA [34], and silicon waveguides [35].

5. Conclusion

Local pump lasers are indispensable for conducting optical signal processing for optical signals. For phase-noise-sensitive advanced modulation formats, the phase noise from local pumps are critical to be considered in order to realize superior optical signal processing. In this chapter, optical signal processing technology for high-order QAM signals has been discussed, with focus on wavelength conversion, wavelength exchange and wavelength multicasting for high-order QAM signals. To design high-performance optical signal processing subsystems, both linear and nonlinear phase noise and distortions are the main concerns in the system design. We first investigated the effective monitoring approach to optimize the performance of wavelength conversion for avoiding undesired nonlinear phase noise and distortions. Then, in the following sections, we discussed our proposed coherent pumping scheme to eliminate the linear phase noise from local pumps in order to realize pump-phase-noise-free wavelength conversion, wavelength exchange and multicasting for high-order QAM signals. Experimental demonstrations were present to verify the feasibility of the proposed coherent pumping schemes.

Acknowledgements

We acknowledge Takahide Sakamoto, Tetsuya Kawanishi, André Albuquerque, Benjamin J. Puttnam, Miguel Drummond, Rogério Nogueira, Atsushi Kanno, Satoshi Shinada, Naoya Wada for their collaborations, and the generous support of Grant-in-Aid for Scientific Research (C) (15K06033), and Grant-in-Aid for Young Scientist (A) (25709031) from the Ministry of Education, Science, Sports and Culture (MEXT), Japan.

Author details

Guo-Wei Lu*

Address all correspondence to: gordon.guoweilu@gmail.com

Tokai University, Japan

References

[1] X. Zhou and J. Yu, "Multi-level, multi-dimensional coding for high-speed and high spectral-efficiency optical transmission," J. Lightw. Technol., 27(16): 3641–3653, 2009.

[2] X. Zhou, J. Yu, M. F. Huang, Y. Shao, T. Wang, L. Nelson, P. D. Magill1, M. Birk, P. I. Borel, D. W. Peckham and R. Lingle "64-Tb/s, 8 b/s/Hz, PDM-36QAM transmission over 320 km using both pre- and post-transmission digital signal processing," J. Lightw. Technol., 29(4): 571–577, 2011.

[3] W. Peng, H. Takahashi, T. Tsuritani, and I. Morita, "DAC-free Generation and 320-km Transmission of 11.2-GBd PDM-64QAM Using a Single I/Q Modulator," in European Conference and Exhibition on Optical Communication, OSA Technical Digest (online) (Optical Society of America, 2012), paper We.1.C.3.

[4] A. Sano, T. Kobayashi, A. Matsuura, S. Yamamoto, S. Yamanaka, E. Yoshida, Y. Miyamoto, M. Matsui, M. Mizoguchi and T. Mizuno "100x120-Gb/s PDM 64-QAM transmission over 160 km using linewidth-tolerant pilotless digital coherent detection," European Conference in Optical Communications, 2010, paper PD2_4.

[5] G.-W. Lu, T. Sakamoto, and T. Kawanishi, "Flexible high-order QAM transmitter using tandem IQ modulators for generating 16/32/36/64-QAM with balanced complexity in electronics and optics," Opt. Express 21: 6213–6223, 2013.

[6] S. R. Nuccio, Z. Bakhtiari, O. F. Yilmaz, and A. Willner, "λ-Conversion of 160-Gbit/s PDM 16-QAM Using a Single Periodically-Poled Lithium Niobate Waveguide," in Optical Fiber Communication Conference/National Fiber Optic Engineers Conference 2011, OSA Technical Digest (CD) (Optical Society of America, 2011), paper OWG5.

[7] T. Richter, R. Nouroozi, H. Suche, W. Sohler, C. Schubert, "PPLN-Waveguide Based Tunable Wavelength Conversion of QAM Data Within the C-Band," IEEE Photonics Technology Letters, IEEE, 25(21): 2085–2088, Nov.1, 2013.

[8] X. Li, J. Yu, Z. Dong, and N. Chi, "Wavelength conversion of 544-Gbit/s dual-carrier PDM-16QAM signal based on the co-polarized dual-pump scheme," Opt. Express 20: 21324–21330, 2012.

[9] A. H. Gnauck, E. Myslivets, M. Dinu, B. P. P. Kuo, P. Winzer, R. Jopson, N. Alic, A. Konczykowska, F. Jorge, J. Dupuy, and S. Radic, "All-Optical Tunable Wavelength Shifting of a 128-Gbit/s 64-QAM Signal," in European Conference and Exhibition on Optical Communication, OSA Technical Digest (online) (Optical Society of America, 2012), paper Th.2.F.2.

[10] B. Filion, S. Amiralizadeh, A. T. Nguyen, L. A. Rusch, and S. LaRochelle, "Wideband Wavelength Conversion of 16 Gbaud 16-QAM Signals in a Semiconductor Optical Amplifier," in Optical Fiber Communication Conference/National Fiber Optic Engineers Conference 2013, OSA Technical Digest (online) (Optical Society of America, 2013), paper OTh1C.5.

[11] G. Contestabile, Y. Yoshida, A. Maruta, and K. Kitayama, "100 nm-Bandwidth Positive-Efficiency Wavelength Conversion for m-PSK and m-QAM signals in QD-SOA," in Optical Fiber Communication Conference/National Fiber Optic Engineers Conference 2013, OSA Technical Digest (online) (Optical Society of America, 2013), paper OTh1C.6.

[12] B. Filion, W. C. Ng, An. T. Nguyen, L. A. Rusch, and S. LaRochelle, "Wideband wavelength conversion of 16 Gbaud 16-QAM and 5 Gbaud 64-QAM signals in a semiconductor optical amplifier," Opt. Express 21: 19825–19833, 2013.

[13] E. Ip, A. P. T. Lau, D. J. F. Barros, and J. M. Kahn, "Coherent detection in optical fiber systems," Opt. Express 16: 753–791, 2008.

[14] Guo-Wei Lu, Takahide Sakamoto, and Tetsuya Kawanishi, "Wavelength conversion of optical 64QAM through FWM in HNLF and its performance optimization by constellation monitoring," Opt. Express 22: 15–22, 2014.

[15] S. Moro, A. Peric, N. Alic, B. Stossel, and S. Radic, "Phase noise in fiber-optic parametric amplifiers and converters and its impact on sensing and communication systems," Opt. Express 18: 21449–21460, 2010.

[16] R. Elschner, and L. Petermann, "Impact of Pump-Induced Nonlinear Phase Noise on Parametric Amplification and Wavelength Conversion of Phase-Modulated Signals," European Conference in Optical Communications, 2009, paper 3.3.4.

[17] T. Richter, R. Elschner, L. Molle, K. Petermann, and C. Schubert, "Coherent Receiver-Based Compensation of Phase Distortions Induced by Single-Pump HNLF-Based FWM Wavelength Converters," in Integrated Photonics Research, Silicon and Nanophotonics and Photonics in Switching, OSA Technical Digest (CD) (Optical Society of America, 2010), paper PWB2.

[18] G. Lu, A. Albuquerque, B. Puttnam, T. Sakamoto, M. Drummond, R. Nogueira, A. Kanno, S. Shinada, N. Wada, and T. Kawanishi, "Pump-linewidth-tolerant optical wavelength conversion for high-order QAM signals using coherent pumps," Opt. Express 22: 5067–5075 (2014).

[19] G. Lu, A. Albuquerque, B. Puttnam, T. Sakamoto, M. Drummond, R. Nogueira, A. Kanno, S. Shinada, N. Wada, and T. Kawanishi, “Pump-Linewidth-Tolerant Optical Data Exchange between 16QAM and QPSK with 50-GHz Channel-Spacing using Coherent DFB Pump,” in Proc. European Conference in Optical Communications, 2010, paper P.2.15.

[20] G. Lu, T. Sakamoto, and T. Kawanishi, "Pump-Phase-Noise-Tolerant Wavelength Multicasting for QAM Signals using Flexible Coherent Multi-Carrier Pump," in Optical Fiber Communication Conference, OSA Technical Digest (online) (Optical Society of America, 2015), paper M2E.2.

[21] K. Uesaka, Kenneth Kin-Yip Wong, M.E. Marhic, Leonid G. Kazovsky, "Wavelength exchange in a highly nonlinear dispersion-shifted fiber: theory and experiments," IEEE Journal of Selected Topics in Quantum Electronics 8(3): 560–568, 2002.

[22] C. H. Kwok, Bill P. P. Kuo, and Kenneth K. Wong, "Pulsed pump wavelength exchange for high speed signal de-multiplexing," Opt. Express 16: 10894–10899, 2008.

[23] Mengzhe Shen, Xing Xu, T.I. Yuk, Kenneth Kin-Yip Wong, "A 160-Gb/s OTDM Demultiplexer Based on Parametric Wavelength Exchange," IEEE Journal of Quantum Electronics 45(11): 1309–1316, 2009.

[24] X. Xu, M. Shen, T. I. Yuk, and K. K. Y. Wong, "Optical Time-Slot Swapping Based on Parametric Wavelength Exchange," in Asia Communications and Photonics Conference and Exhibition, Technical Digest (CD) (Optical Society of America, 2009), paper TuC1.

[25] Jian Wang, Zahra Bakhtiari, Omer F. Yilmaz, Scott Nuccio, Xiaoxia Wu, and Alan E. Willner, "10 Gbit/s tributary channel exchange of 160 Gbit/ssignals using periodically poled lithium niobate," Opt. Lett. 36: 630–632, 2011.

[26] Jian Wang, Zahra Bakhtiari, Scott R. Nuccio, Omer F. Yilmaz, Xiaoxia Wu, and Alan E. Willner, "Phase-transparent optical data exchange of 40 Gbit/s differential phase-shift keying signals," Opt. Lett. 35: 2979–2981; 2010.

[27] Yingying Xu, Juhao Li, Paikun Zhu, Bingli Guo, Yuanxiang Chen, Yucheng Zhong, Yan Wang, Zhangyuan Chen, and Yongqi He, “Demonstration of All-optical Inverse Multiplexing in Elastic Optical Networks,” in Optical Fiber Communication Conference (2014), paper Th1E.6,

[28] G.-W. Lu, K. S. Abedin, and T. Miyazaki, “DPSK multicast using multiple-pump FWM in Bismuths highly nonlinear fiber with high multicast efficiency,” Opt. Express 16(26): 21964–21970, 2008.

[29] C. Zhiyu, Y. Lianshan, P. Wei, L. Bin, Y. Anlin, G. Yinghui, and L. Ju Han, “One-to-nine multicasting of RZ-DPSK based on cascaded four-wave mixing in a highly nonlinear fiber without stimulated Brillouin scattering suppression,” IEEE Photon. Technol. Lett. 24(20): 1882–1885, 2012.

[30] M. P. Fok and C. Shu, “Multipump four-wave mixing in a photonic crystal fiber for 6 ×10 Gb/s wavelength multicasting of DPSK signals,” IEEE Photon. Technol. Lett. 19(15): 1166–1168, 2007.

[31] M. Pu, H. Hu, H. Ji, M. Galili, L. K. Oxenløwe, P. Jeppesen, J. M. Hvam, and K. Yvind, “One-to-six WDM multicasting of DPSK signals based on dual-pump four-wave mixing in a silicon waveguide,” Opt. Express 19(24): 24448–24453, 2011.

[32] W. Dawei, C. Tee-Hiang, Y. Yong-Kee, X. Zhaowen, W. Yixin, X. Gaoxi, and L. Jian-guo, “Performance comparison of using SOA and HNLF as FWM medium in a wavelength multicasting scheme with reduced polarization sensitivity,” J. Lightwave Technol. 28(24): 3497–3505, 2010.

[33] W. Shief, “Maximum-likelihood phase and channel estimation for coherent optical OFDM,” Photon. Technol. Lett., 20(8), 605, 2008.

[34] Jun Qin, Guo-Wei Lu, Takahide Sakamoto, Kouichi Akahane, Naokatsu Yamamoto, Danshi Wang, Cheng Wang, Hongxiang Wang, Min Zhang, Tetsuya Kawanishi, and Yuefeng Ji, "Simultaneous multichannel wavelength multicasting and XOR logic gate multicasting for three DPSK signals based on four-wave mixing in quantum-dot semiconductor optical amplifier," Opt. Express 22: 29413–29423, 2014.

[35] Mohammadreza Khorasaninejad and Simarjeet Singh Saini, "Silicon nanowire optical waveguide (SNOW)," Opt. Express 18: 23442–23457, 2010.

IntechOpen

IntechOpen

IntechOpen